

Electronic Supplementary Information (ESI)

**Unlocking the capacity of iodide for high-energy-density
zinc/polyiodide and lithium/polyiodide redox flow batteries**

Guo-Ming Weng, Zhejun Li, Guangtao Cong, Yucun Zhou and Yi-Chun Lu*

Electrochemical Energy and Interfaces Laboratory, Department of Mechanical and Automation
Engineering, The Chinese University of Hong Kong, Shatin, N. T. 999077, Hong Kong SAR, China

*E-mail: yichunlu@mae.cuhk.edu.hk

Experimental details

Computational method of bonding length of polyhalide ions. Plane wave based VASP code was employed to conduct the first-principles density functional theory calculations. Perdew-Burke-Ernzerhof (PBE) version of the generalized gradient approximation (GGA) and projector augmented wave (PAW) pseudopotentials were used to model the electronic exchange correlation effect^{1, 2}.

Preparation and assembly of aqueous zinc/iodine-bromide batteries (ZIBB). The configuration and photographs of the components of the ZIBB single cell are shown in Fig. 1e and Fig. S2. In each half-cell, a piece of graphite felt (GF, 3 mm thickness and active geometric area of 4 cm², Yi Deshang Carbon Technology Co. Ltd., China) was used as the electrode and a graphite plate (Beijing Jing Long Te Tan Co. Ltd., China) was used as the current collector. The GFs are pretreated with acid prior to cell assembling³. The compression of GFs was controlled by utilizing a 2-mm-thick PTFE frame (as shown in Fig. S2, the rectangle part of the frame), compressing each GF electrode to c.a. 66% of their initial thickness in the assembled cell. The Zn²⁺-form Nafion membranes (N-115 and N-117 from Dupont, USA, active area of 4 cm²) were pretreated prior to use with the following steps: i) The Nafion membrane was soaked in 3 wt% H₂O₂ aqueous solution at 60 °C for 1 hour. It was rinsed with deionized (DI) water to remove the remaining H₂O₂; ii) The Nafion membrane was soaked in 0.5 M H₂SO₄ at 60 °C for 1 hour and rinsed with DI water until pH in the effluent is near 7; iii) It was soaked in 1 M ZnCl₂ aqueous solution (pH was adjusted to 1 by using HCl) at 60 °C for 3 hours to convert from the H⁺-form to the Zn²⁺-form. Then the membrane was rinsed with DI water and stored in DI water. The electrolytes with different concentrations were prepared by dissolving corresponding ZnI₂ (Jindian Chemical Co. Ltd., China, 99%) and ZnBr₂ (Xinbao Fine Chemical Factory, 98%) in an Argon (Ar)-saturated DI water in an Ar-filled glove box (Etelux, H₂O < 1.0 ppm, O₂ < 1.0 ppm).

For the flow batteries used in the galvanostatic test (shown in Fig. 1f and Fig. S5), one single N-115 Nafion membrane was used as separator. For the flow ZIBB used in the cycle test (shown in Fig. 3, two N-117 Nafion membranes and one hydrophilic porous paper (placed between membranes and negative electrode, c.a. 4.2 cm², thickness of 205 μm, pore size of 20~25 μm, Whatman, #1004-047) were used as separator to reduce crossover and provide space for the zinc formation⁴. This is because of: i) Donnan exclusion becomes weaker and thus lower perm-selectivity of the ion-exchange membrane in highly concentrated electrolyte solution. Thicker membrane was found to show less crossover and better capacity retention ability³; ii) The presence of porous paper could alleviate the dendrite growth of the zinc metal; iii) The presence of porous paper could further enhance the plating utilization of porous carbon electrode⁵.

Preparation of Li_{1.5}Al_{0.5}Ge_{1.5}(PO₄)₃ ceramic membrane. The lithium ion conductor,

Li_{1.5}Al_{0.5}Ge_{1.5}(PO₄)₃ (LAGP), was synthesized using a modified solid-state reaction method⁶ and used as the separator for the nonaqueous lithium/iodine-bromide battery (LIBB). Briefly, LiOH·H₂O (Sinopharm Chemical Reagent Co. Ltd., China, 95%), Al₂O₃ (gamma phase, <50 nm, Sigma-Aldrich, # 544833), GeO₂ (Sinopharm Chemical Reagent Co. Ltd., China, 99.999%), and NH₄H₂PO₄ (Sinopharm Chemical Reagent Co. Ltd., China, 99%) were used as the starting materials. The precursors were thoroughly mixed by planetary ball milling at 400 rpm for 12 hours in acetone and then heated at 600 °C for 2 hours. The mixture was then cooled, ball milled and heated at 800 °C for 6 hours. After that, the obtained powder was mixed thoroughly again with ball milling process at 400 rpm for 12 hours in acetone and the dried powder was pressed into pellets and sintered at 850 °C for 6 hours. The diameter of the final product is 16 mm.

Preparation and assembly of nonaqueous lithium/iodine-bromide batteries (LIBB). The configuration and the components of a nonaqueous lithium/iodine-bromide battery (LIBB) are shown in the Fig. S8 and described in our previous works ^{7,8}. To assembly the LIBB: i) One piece of lithium foil (immersed in

0.1 M LiNO₃ of DOL:DME (1:1 v:v) overnight before use) was pressed onto the inner surface of the stainless steel bottom casing; ii) Two Celgard 2325 separators were placed on the lithium foil and total 120 μ L negative electrolyte, 0.2 M LiClO₄-0.1 M LiNO₃ in DOL:DME (1:1 v:v), was added on the separators; iii) One piece of LAGP was placed on the Celgard separators; iv) One piece of carbon paper (Shanghai Hesen Co. Ltd., China, #HCP020N, thickness is 0.2 mm and geometric active area is 1.13 cm²) was placed on the LAGP to serve as both positive electrode and buffer layer; v) 10 μ L positive electrolyte, 2.5 M LiI or 2.5 M LiI + 1.25 M LiBr in DOL:DME (1:1 v:v), was added on this carbon paper; vi) Additional piece of carbon paper was placed on the 1st carbon paper to act as current collector followed by a stainless steel spring; vii) Two casings (bottom and top) were separated by a polytetrafluoroethylene (PTFE) spacer and the assembly was conducted in the Ar-filled glove box. The electrolytes were prepared by dissolving LiI (Acros, 99%), LiBr (Kermel, AR), LiClO₄ (Sigma Aldrich, 99+%) and LiNO₃ (Sigma Aldrich, 99.99%) in the binary solvents of 1,3-Dioxolane (DOL) (Sigma Aldrich, anhydrous, 99.8%) and 1,2-Dimethoxyethane (DME) (Sigma Aldrich, anhydrous, 99.5%). The thickness of the LAGP used in the galvanostatic test of LIBB and iodide-only lithium battery (shown in Fig. 4) was 0.63 \pm 0.04 mm.

Test of static and flow batteries. Experiments of charge/discharge test and AC impedance were carried out with a Bio-logic VMP3 potentiostat at 20 °C. The charge and discharge tests of the ZIBB are operated with constant current method (current density is based on the active geometric area of the electrode) and the charge process was controlled by both voltage and capacity while the cutoff voltage of discharge was varied from 0.3 to 0.6 V. All ZIBB cells were balanced by using equal volume of electrolyte for each half-cell and, typically, 1 mL of electrolyte was circulated by a peristaltic pump (Cole Parmer, 7528-20 with Masterflex 77390-00 PTFE pump head) at the same flow rate in each half-cell through PTFE tubing for the flow ZIBB cell. For the test of LIBB, the current density is based on the geometric active area of the carbon paper electrode. The cutoff voltages for the typical charge and discharge cycle are 3.2 V and 2.4 V, while those in the cycle test are 3.25 V and 2.5 V. For the discharge polarization test (Fig.

2b), the ZIBB was first pre-charged at 5 mA cm^{-2} with a cutoff at 1.5 V, this cell was then discharged at the specified current density for 30 s and followed 1 min relaxation at its OCV. This process was repeated with stepwise increase in current density. The corresponding potential plotted in the discharge polarization curve (Fig. 2b) was the average discharge voltage over a 30 s period at each current step.

Characterization. Electrospray ionization mass spectra (ESI-MS) were collected by using Q Exactive Focus Hybrid Quadrupole-Orbitrap Mass Spectrometer with HESI II source in negative ion mode. The cyclic voltammetry was carried out with Bio-logic VMP3. CVs (Fig. 1d and Fig. S1) were measured via a glassy carbon (active area of 0.07 cm^2), Pt wire and SCE (filling solution is saturated KCl, 0.241 V vs. SHE) were used as working, counter and reference electrodes, respectively. Four-electrode characterization³ was conducted by inserting a SCE reference electrode into each half-cell and the setup is shown in Fig. S9.

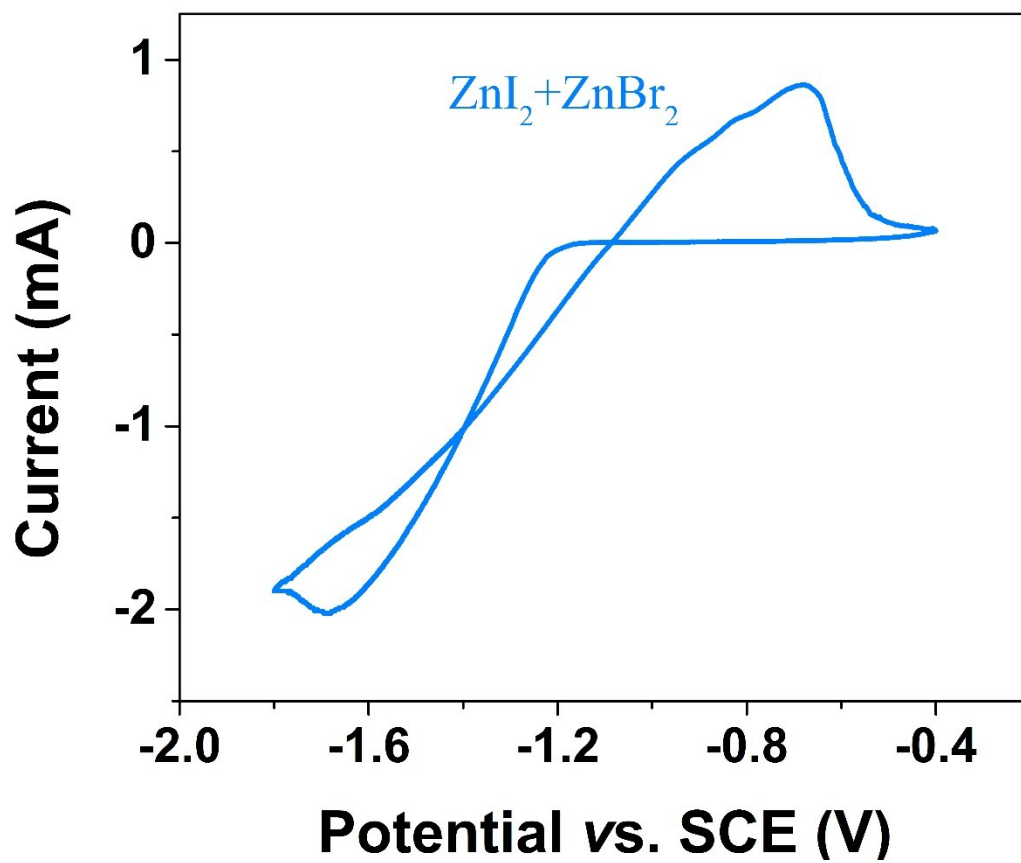


Figure S1. Cyclic voltammograms of 0.1 M ZnI₂ + 0.05 M ZnBr₂ at the scan rate of 50 mV s⁻¹.

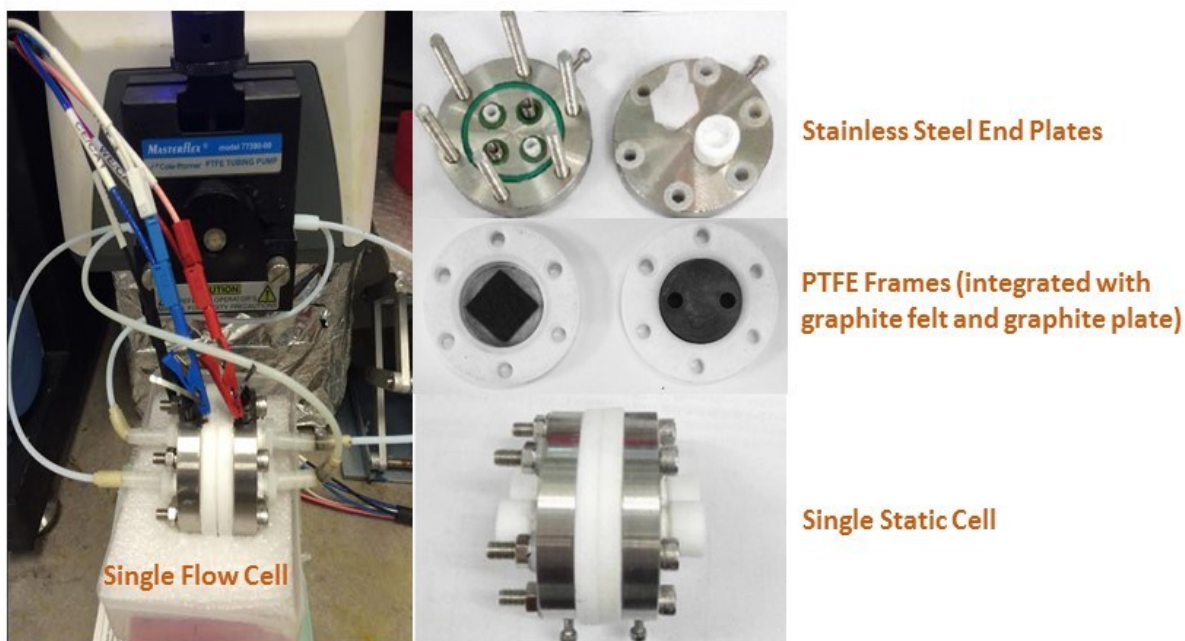


Figure S2. Photographs of components of a single ZIBB cell.

Table S1. Thermodynamic data on halides in aqueous state. All data is obtained from ref. 9.

Species	I ⁻	Br ⁻	I ₃ ⁻	I ₂ Br ⁻	I _{2(aq)}	Zn	Zn ²⁺
$\Delta G^\circ / \text{kJ mol}^{-1}$	-51.67	-103.97	-51.50	-92.596	16.43	0	-147.16

Note: Calculation of standard electrode potential. The theoretical standard electrode potential of the reaction shown in eq. 1, eq. 4, and eq. 5 (see main text) is determined to be 0.621 V_{SHE}, 0.536 V_{SHE}, and 0.594 V_{SHE} following $\Delta G^\circ = -nFE^\circ$, where ΔG° is the free energy of the reaction, n is the number of moles of electrons being transferred, F stands for the Faraday constant (96485 C mol⁻¹) and E° is the standard potential of the reaction.



Solid ZnI_2 precipitation is observed at 5.6 M ZnI_2 at room temperature

Figure S3. Photograph of a 50 mL 5.6 M ZnI_2 aqueous solution at room temperature.

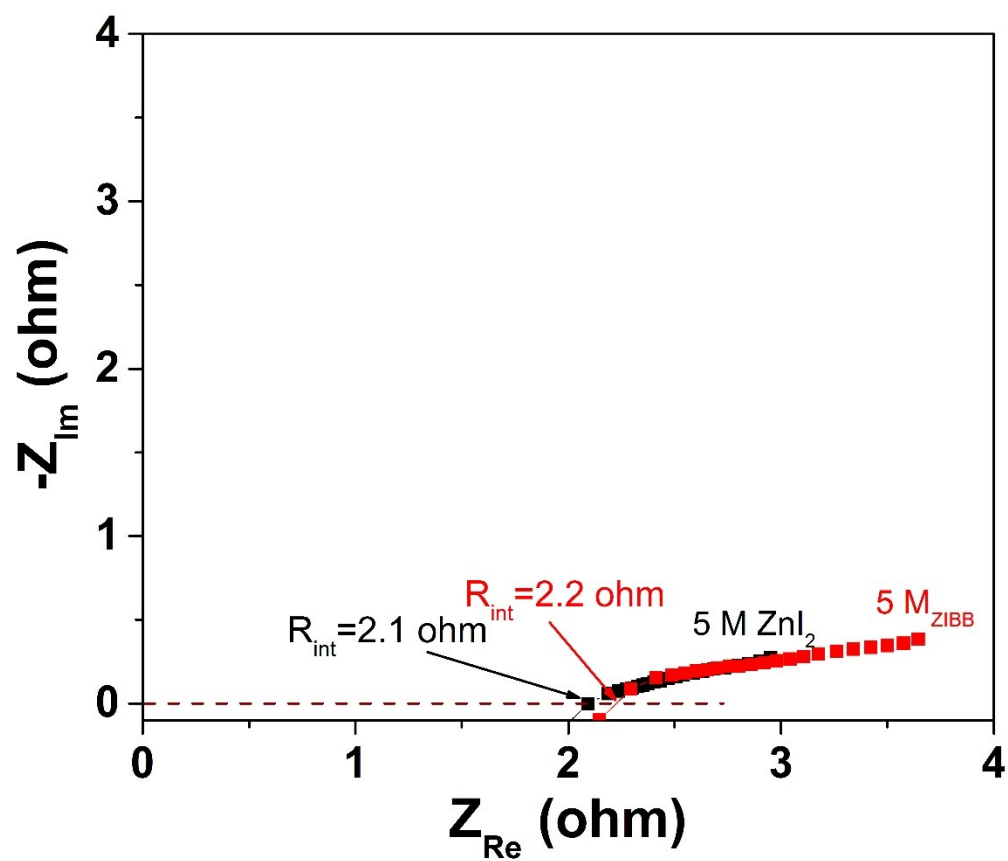


Figure S4. AC impedance test of the 5 M ZIBB (5.0 M ZnI_2 + 2.5 M $ZnBr_2$) and 5 M ZIB (5.0 M ZnI_2) flow systems with N-115 at a flow rate of 10 mL min^{-1} . Before each test, the cell is rested for 1 hour.

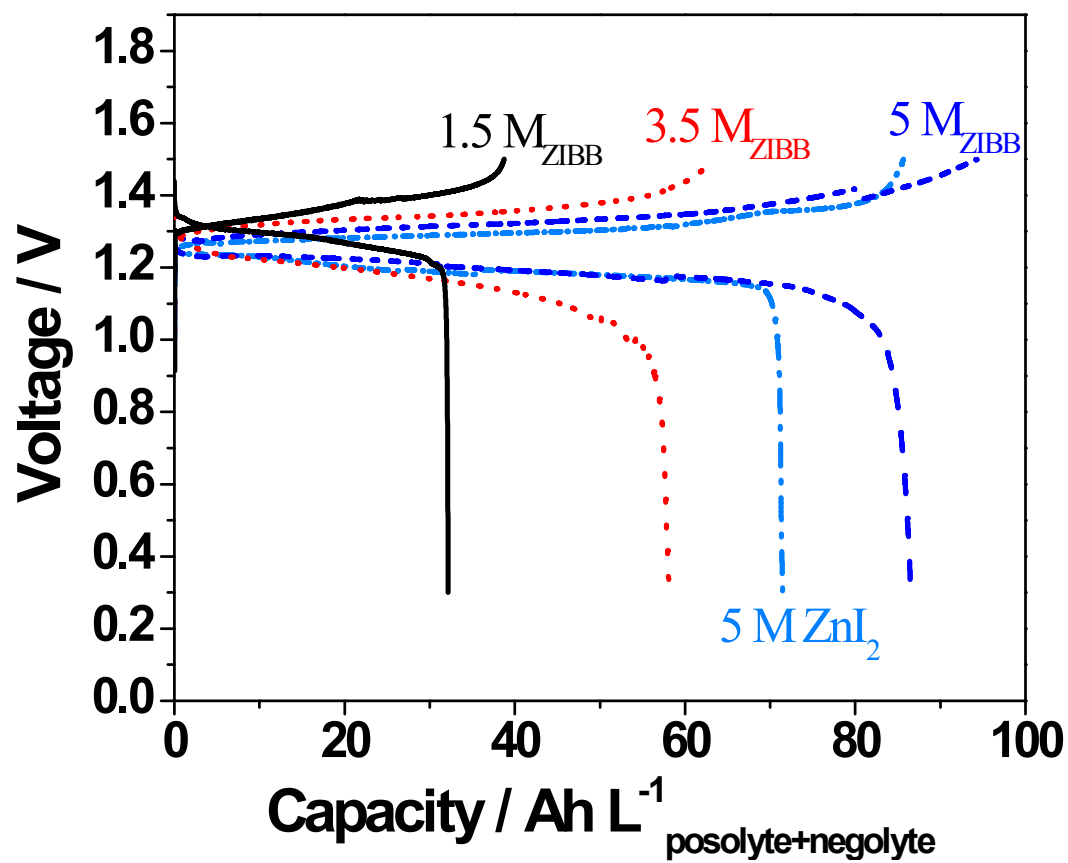


Figure S5. Galvanostatic voltage profiles of the ZIBB systems at various concentrations at a flow rate of 10 mL min⁻¹. The charge/discharge current density is 5 mA cm⁻².

Table S2. Characteristics of aqueous redox flow batteries

Systems	Ref.	Electrochemistry	$\Delta E^{\circ}_{\text{cell}}$	Theoretical specific energy*, Wh kg ⁻¹	Demonstrated maximum volumetric energy density**, Wh L ⁻¹
<i>Typical systems</i>					
Fe/Cr	10	+ve: $\text{Fe}^{3+} + \text{e}^- \xrightleftharpoons[\text{charge}]{\text{discharge}} \text{Fe}^{2+}$ $(E^{\circ}=0.77 \text{ V})$ -ve: $\text{Cr}^{2+} \xrightleftharpoons[\text{charge}]{\text{discharge}} \text{Cr}^{3+} + \text{e}^-$ $(E^{\circ}=-0.41 \text{ V})$	1.18	99	12.8
VRF (3 M)	11	+ve: $\text{VO}_2^+ + 2\text{H}^+ + \text{e}^- \xrightleftharpoons[\text{charge}]{\text{discharge}} \text{VO}^{2+} + \text{H}_2\text{O}$ ($E^{\circ}=1.00 \text{ V}$) -ve: $\text{V}^{2+} \xrightleftharpoons[\text{charge}]{\text{discharge}} \text{V}^{3+} + \text{e}^-$ $(E^{\circ}=-0.26 \text{ V})$	1.26	60.5	50.6
VRF (mixed acid)	12	+ve: $\text{VO}_2^+ + 2\text{H}^+ + \text{e}^- \xrightleftharpoons[\text{charge}]{\text{discharge}} \text{VO}^{2+} + \text{H}_2\text{O}$ ($E^{\circ}=1.00 \text{ V}$) -ve: $\text{V}^{2+} \xrightleftharpoons[\text{charge}]{\text{discharge}} \text{V}^{3+} + \text{e}^-$ $(E^{\circ}=-0.26 \text{ V})$	1.26	60.5	43.1
ZBB	13	+ve: $\text{Br}_2 + 2\text{e}^- \xrightleftharpoons[\text{charge}]{\text{discharge}} 2\text{Br}^-$ $(E^{\circ}=1.00 \text{ V})$ -ve: $\text{Zn} \xrightleftharpoons[\text{charge}]{\text{discharge}} \text{Zn}^{2+} + 2\text{e}^-$ $(E^{\circ}=-0.76 \text{ V})$	1.76	209.4	61.5
<i>Novel systems</i>					
AQS/Br	14	+ve: $\text{Br}_2 + 2\text{e}^- \xrightleftharpoons[\text{charge}]{\text{discharge}} 2\text{Br}^-$ $(E^{\circ}=1.00 \text{ V})$ -ve: $\text{H}_2\text{AQS} \xrightleftharpoons[\text{charge}]{\text{discharge}} \text{AQS} + 2\text{H}^+ + 2\text{e}^-$ ($E^{\circ}=+0.09 \text{ V}$)	0.91	85	16.5
ZIB	15	+ve: $\text{I}_3^- + 2\text{e}^- \xrightleftharpoons[\text{charge}]{\text{discharge}} 3\text{I}^-$ ($E^{\circ}=0.536 \text{ V}$) -ve: $\text{Zn} \xrightleftharpoons[\text{charge}]{\text{discharge}} \text{Zn}^{2+} + 2\text{e}^-$ $(E^{\circ}=-0.76 \text{ V})$	1.296	87.1	166.7 (posolyte)

Zn/Tempo	16	$\text{+ve: TEMPO}^+ + \text{e}^- \xrightleftharpoons[\text{charge}]{\text{discharge}} \text{TEMPO}$ $(E^0=0.93 \text{ V})$ $\text{-ve: Zn} \xrightleftharpoons[\text{charge}]{\text{discharge}} \text{Zn}^{2+} + 2\text{e}^-$ $(E^0=-0.76 \text{ V})$	1.69	203	2-4
V/MH-H ₂	3	$\text{+ve: VO}_2^+ + 2\text{H}^+ + \text{e}^- \xrightleftharpoons[\text{charge}]{\text{discharge}} \text{VO}^{2+}$ $+ \text{H}_2\text{O} (E^0=1.00 \text{ V})$ $\text{-ve: MH}_x + \text{OH}^- \xrightleftharpoons[\text{charge}]{\text{discharge}} \text{MH}_{x-1} +$ $\text{H}_2\text{O} + \text{e}^- (E^0=-0.80 \text{ V})$	1.80	200/300	2-3
TEMPO/ Viol	17	$\text{+ve: TEMPO}^+ + \text{e}^- \xrightleftharpoons[\text{charge}]{\text{discharge}} \text{TEMPO}$ $(E^0=0.93 \text{ V})$ $\text{-ve: Viol}^+ \xrightleftharpoons[\text{charge}]{\text{discharge}} \text{Viol}^{2+} + \text{e}^- (E^0=-$ $0.17 \text{ V})$	1.1	86.1	10
Br ⁻ -Cl ⁻ /VCl ₃	18	$\text{+ve: BrCl}_2^- + 2\text{e}^- \xrightleftharpoons[\text{charge}]{\text{discharge}} \text{Br}^- + 2\text{Cl}^-$ $(E^0=1.04 \text{ V})$ $\text{-ve: V}^{2+} \xrightleftharpoons[\text{charge}]{\text{discharge}} \text{V}^{3+} + \text{e}^-$ $(E^0=-0.26 \text{ V})$	1.3	78	-
ZIBB	<i>This work</i>	$\text{+ve: I}_2\text{Br}^- + 2\text{e}^- \xrightleftharpoons[\text{charge}]{\text{discharge}} 2\text{I}^- + \text{Br}^-$ $(E^0=0.54 \text{ V})$ $\text{-ve: Zn} \xrightleftharpoons[\text{charge}]{\text{discharge}} \text{Zn}^{2+} + 2\text{e}^-$ $(E^0=-0.76 \text{ V})$	1.3	96.7	101 202 (posolyte)

Notes: * Most values of specific energy are obtained from Ref. 19.

** All volumetric cell capacity and energy density are based on both electrolyte volumes,

except for those specified. Most values of volumetric energy density are obtained from Ref. 15.

Supplementary Note: Abbreviations of flow batteries in Supplementary Table S2.

Fe/Cr: Iron/Chromium Flow Battery

VRF: All Vanadium Redox Flow Battery

ZBB: Zinc/Bromine Flow Battery

AQS/Br: 9,10-anthraquinone-2,7-disulfonic acid/Bromine flow battery

ZIB: Zinc/Polyiodide Flow Battery

Zn/Tempo: Zinc/(Tetramethylpiperidine 1-oxyl) Flow Battery

V/MH-H₂: Vanadium/Metal hydride-hydrogen Flow Battery

Tempo/Viol: (Tetramethylpiperidine 1-oxyl)/(4,4'-bipyridine derivative) Flow Battery

Br-Cl/VCl₃: Polyhalide/Vanadium Flow Battery

ZIBB: Zinc/Iodine-bromide Flow Battery

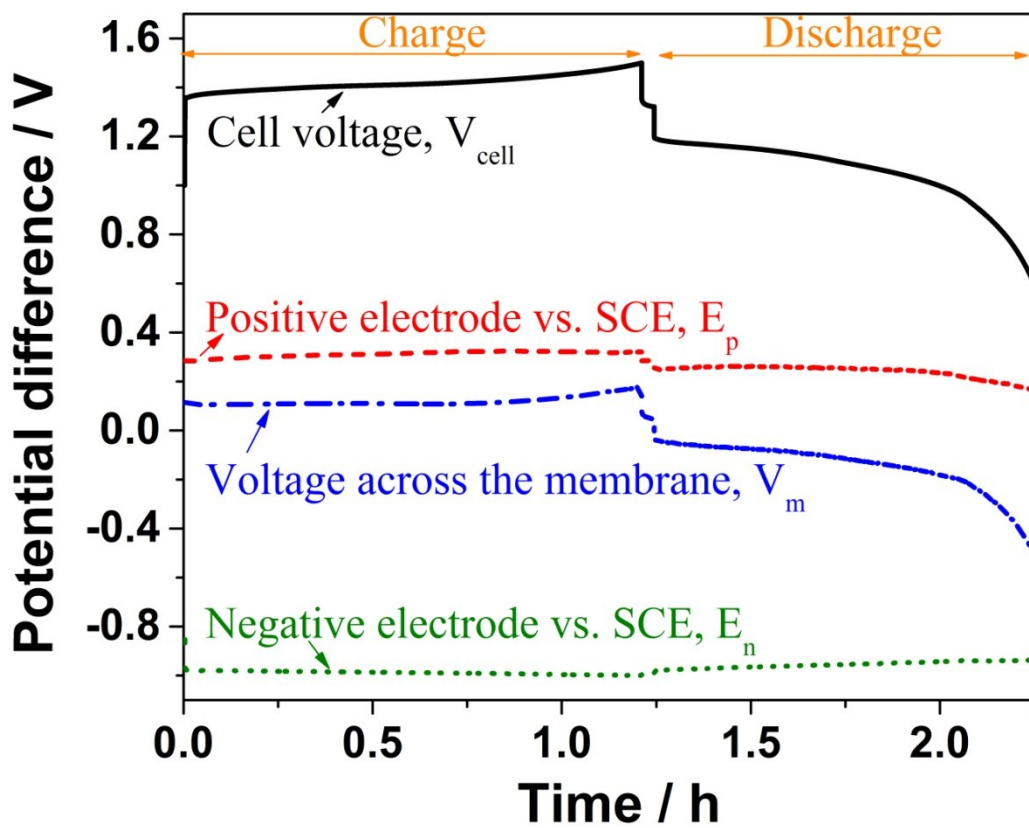


Figure S6. Four-electrode characterization of a ZIBB system (3.5 M ZnI_2 + 1.75 M $ZnBr_2$) with one N-115 Nafion membrane at 15 mA cm^{-2} .

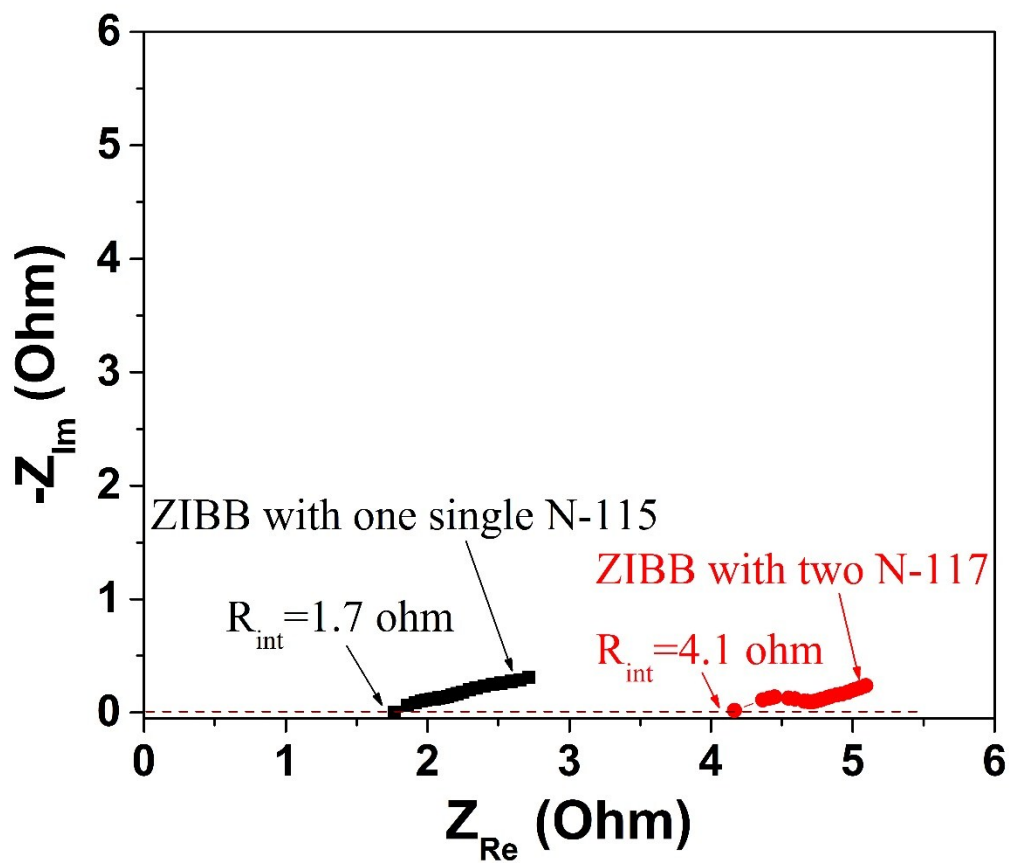


Figure S7. AC impedance test of ZIBB systems (3.5 M ZnI_2 + 1.75 M $ZnBr_2$) with one single N-115 Nafion and two N-117 Nafion membranes. The flow rate is fixed at 10 mL min^{-1} . Before each test, the cell is rested for 1 hour.

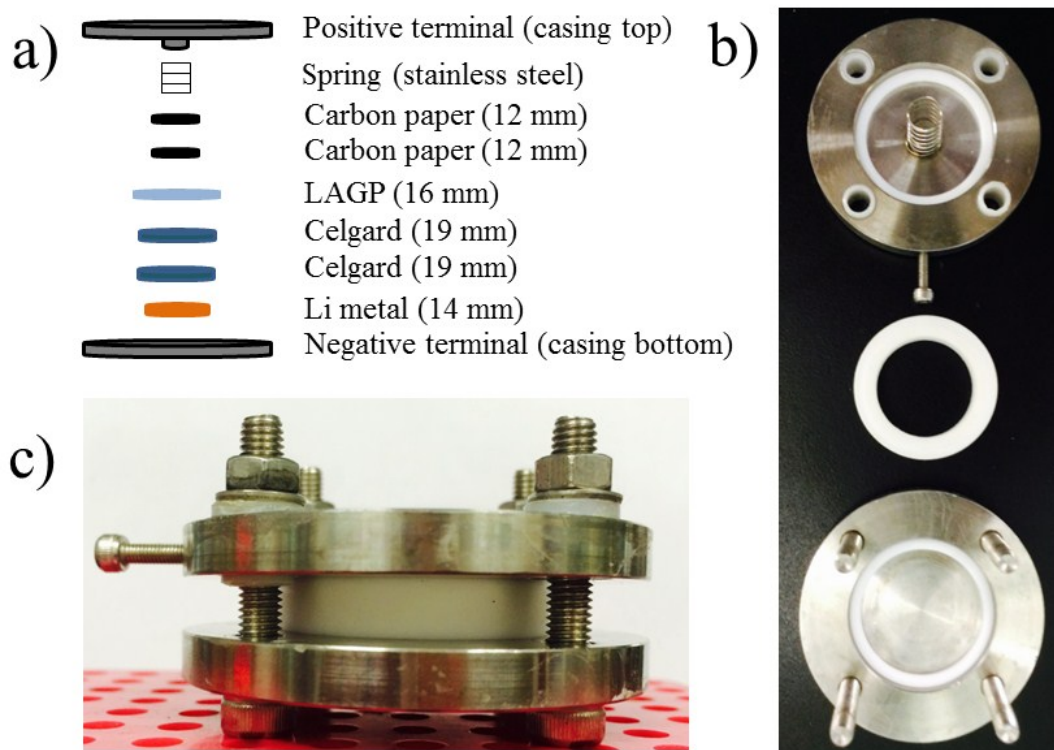


Figure S8. Schematic representation and photographs of the LIBB cell.

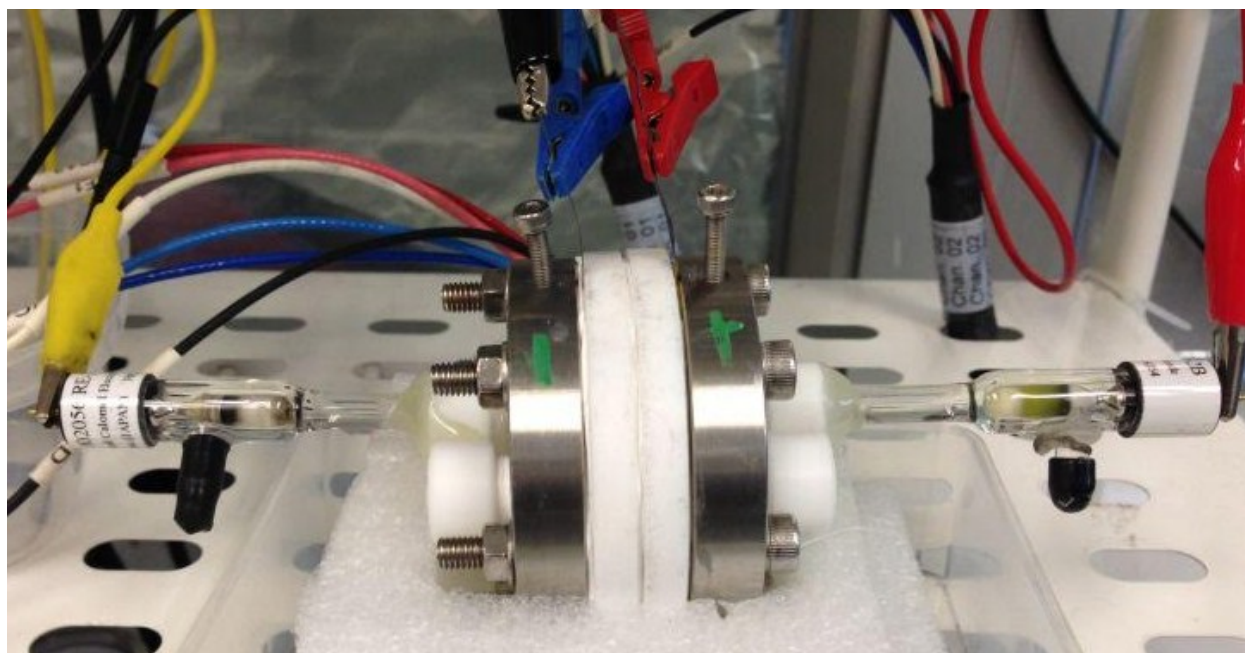


Figure S9. The photograph of the experimental setup of the four-electrode characterization.

Supplementary References

1. G. Kresse and J. Furthmüller, *Phys. Rev. B*, 1996, **54**, 11169.
2. G. Kresse and J. Furthmüller, *Comput. Mater. Sci.*, 1996, **6**, 15-50.
3. G. M. Weng, C. Y. V. Li, K. Y. Chan, C. W. Lee and J. Zhong, *J. Electrochem. Soc.*, 2016, **163**, A5180-A5187.
4. J. L. Devitt and D. H. McClelland, *Separators for secondary alkaline batteries having a zinc-containing electrode, U.S. Patent 3,669,746 (1972)*.
5. N. C. Hoyt, K. L. Hawthorne, R. F. Savinell and J. S. Wainright, *J. Electrochem. Soc.*, 2016, **163**, A5041-A5048.
6. H. Kitaura and H. Zhou, *Energy Environ. Sci.*, 2012, **5**, 9077-9084.
7. H. Chen and Y. C. Lu, *Adv. Energy Mater.*, 2016, 1502183.
8. H. Chen, Q. Zou, Z. Liang, H. Liu, Q. Li and Y.-C. Lu, *Nat. Commun.*, 2015, **6**, 5877.
9. A. J. Bard, R. Parsons and J. Jordan, *Standard potentials in aqueous solution*, CRC press, 1985.
10. L. H. Thaller, *Energy storage system, U.S. Patent 3,996,064 (1976)*.
11. S. Roe, C. Menictas and M. Skyllas-Kazacos, *J. Electrochem. Soc.*, 2016, **163**, A5023-A5028.
12. L. Li, S. Kim, W. Wang, M. Vijayakumar, Z. Nie, B. Chen, J. Zhang, G. Xia, J. Hu and G. Graff, *Adv. Energy Mater.*, 2011, **1**, 394-400.
13. A. Z. Weber, M. M. Mench, J. P. Meyers, P. N. Ross, J. T. Gostick and Q. Liu, *J. Appl. Electrochem.*, 2011, **41**, 1137-1164.
14. B. Huskinson, M. P. Marshak, C. Suh, S. Er, M. R. Gerhardt, C. J. Galvin, X. Chen, A. Aspuru-Guzik, R. G. Gordon and M. J. Aziz, *Nature*, 2014, **505**, 195-198.
15. B. Li, Z. Nie, M. Vijayakumar, G. Li, J. Liu, V. Sprenkle and W. Wang, *Nat. Commun.*, 2015, **6**, 6303.
16. J. Winsberg, T. Janoschka, S. Morgenstern, T. Hagemann, S. Muench, G. Hauffman, J. Gohy, M. D. Hager and U. S. Schubert, *Adv. Mater.*, 2016, 201505000.
17. T. Janoschka, N. Martin, U. Martin, C. Friebe, S. Morgenstern, H. Hiller, M. D. Hager and U. S. Schubert, *Nature*, 2015, **527**, 78-81.
18. M. Skyllas-Kazacos, *J. Power Sources*, 2003, **124**, 299-302.
19. G. M. Weng, C. Y. V. Li and K. Y. Chan, *J. Electrochem. Soc.*, 2013, **160**, A1384-A1389.